01

Peculiarities of Fluorescence of Rb Atomic Vapors Contained in a cell with an anti-relaxation coating

© A. Sargsyan, A. Papoyan, D. Sarkisyan

Institute of Physical Research fot the National Academy of Sciences of Armenia,
0203 Ashtarak, Armenia

e-mail: sargsyanarmen85@gmail.com

Received: February 02, 2023
Revised: February 02, 2023
Accepted: February 13, 2023

The features of the fluorescence spectra of Rb D_1-line vapors were studied for the first time using a cell with anti-relaxation PolyDiMethylSiloxane (PDMS) coating. At high intensities ($> 200\,\mathrm{mW/cm^2}$) of a cw narrow-band diode laser in the transmission spectra due to the effect of optical pumping, there are no absorption lines at atomic transitions, while in the fluorescence spectrum, all 8 atomic transitions of the D_1 line are pronounced. A strong redistribution of fluorescence intensity is registered for atomic transitions of ^{85}Rb and ^{87}Rb: in particular, the ratio of fluorescence amplitudes for transitions of ^{87}Rb $F_g = 1 \rightarrow F_e = 1, 2$ in a regular cell is 5, while for a PDMS cell it is equal to 1.5. A physical explanation of the observed features of fluorescence in a PDMS cell is given. A significant increase of fluorescence intensity and a change in redistribution at the transitions with increasing of the PDMS cell temperature is demonstrated. It is noted that at large intensities of laser radiation (when there are no peaks on the transmission/absorption spectra of atomic transitions), fluorescence spectra remain the only convenient and informative tool for studying the behavior of atoms.

Keywords: Rubidium atoms, alkali metals, antirelaxation coating, optical pumping, absorption and fluorescence of atomic vapors.

DOI: 10.61011/EOS.2023.02.55794.4585-22

Introduction

Vapor of alkali metal atoms enclosed in glass, quartz, and sapphire cells are widely used in laser physics [1]. This is due to strong atomic transitions in the near-IR region, with availability of lasers with good parameters, and the ease of obtaining large atomic densities. Therefore, work continues on cell modernization. For example, cells with vapor column thicknesses of several hundred of nanometers have been shown to be a convenient tool for studying atomic transitions, particularly in strong magnetic fields [2,3]. To exclude inelastic collisions of atoms with cell walls, which leads to atom spin randomization due to atom-surface collisions, anti-relaxation organic coatings are applied to the cell walls. In this case, the $\langle \mathbf{S} \cdot \mathbf{I} \rangle$ operator gives the main contribution to the spin dynamics [4–8]. In other words, thanks to organic coatings such as siloxane, paraffin or polydimethylsiloxane (PDMS) films, the $\langle \mathbf{S} \cdot \mathbf{I} \rangle$ operator does not change in time for tens of seconds or more [9]. Because of their remarkable spin conservation properties, organic coatings have been successfully applied in magnetometry, laser cooling, atom capturing, coherent processes, etc. [10–14]. It has been found in [15–18] that the anti-relaxation coating also accumulates significant amounts of alkali metal atoms, which can be easily released by non-resonant blue or violet light due to a process called light-induced atomic desorption (LIAD).

In work [19], it is shown that the use of a PDMS-coated cell strongly modifies the spectrum of electromagnetically induced transparency (EIT) resonances in vapor of Rb atoms in a magnetic field. Two of the four EIT resonances show a decrease in absorption, while the other two show an increase in absorption. In an uncoated cell, all four EIT resonances show a decrease in absorption.

In work [20], it was shown that in the presence of organic coatings of paraffin or PDMS deposited on the cell walls, the absorption spectra of Rb vapor line D_2 register the redistribution of the population created by optical pumping. In particular, deformation of absorption profiles and frequency shift of peak amplitudes were observed, and these changes are strongly dependent on the speed and direction of laser frequency scanning. It was shown that the coated cell significantly exhibited hyperfine optical pumping when the laser intensity was increased, leading to a decrease in absorption at atomic transitions by a factor of tens.

In common cells with alkali metal vapor, the absorption and fluorescence spectra are almost identical [21]. The difference between these spectra was recorded only for cells having a nanometer thickness in the direction of laser radiation propagation [22]: the spectral absorption width reaches a minimum value at $L = (2n + 1)\lambda/2$ (where n — an integer, λ — the wavelength of the laser radiation with a frequency resonant to the corresponding transition), while the spectral width of fluorescence reaches a minimum value at $L = \lambda/2$ and increases monotonically with increasing L up to the Doppler width at $L \sim 5\,\mu$m.

In the present work, the fluorescence (FL) spectra of the Rb vapor D_1 line using a PDMS-coated cell were investigated for the first time and a significant difference with the absorption spectrum was registered.

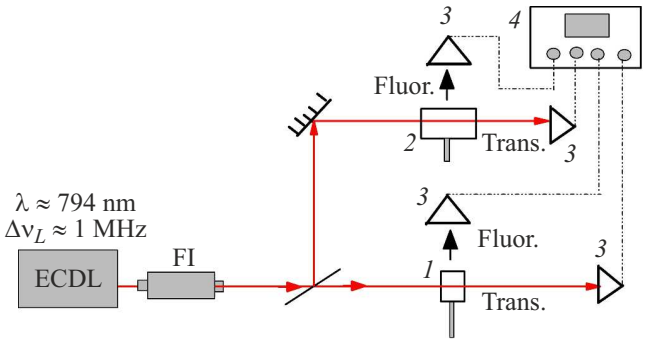

Figure 1. Experimental scheme for recording the absorption and FL spectra of a PDMS cell: ECDL — tunable diode laser $\lambda = 795$ nm, FI — Faraday insulator, *1* — 8 mm PDMS coated cell, *2* — additional Rb cm cell, *3* — FD-24K photodiodes, *4* — Tektronix TDS 2024C Oscilloscope

1. Experiment

Fig. 1 shows the experimental scheme for recording the absorption and fluorescence spectra of the PDMS-coated cell. We used an extended cavity diode laser (ECDL) with a wavelength of 795 nm, spectral width of ~ 1 MHz, and a beam diameter of 1.5 mm. The scanning frequency of the laser was fixed at 50 Hz. Faraday FI isolator was used to prevent feedback. Laser radiation with a power P between $10\,\mu$W-10 mW was directed to an 8 mm-glass cell (*1*) coated with PDMS, filled with Rb vapor, which was at room temperature. Optical emissions were detected by photodiodes (FD-24K (*3*), whose signals were amplified and fed to a Tektronix TDS2014B (*4*) four-channel oscilloscope. Photodiodes simultaneously recorded the radiation and FL passing through the cell. A large usable aperture of 10 mm diameter makes it convenient to register fluorescence laterally with the FD-24K photodetector, which is located close to the cell. To form a frequency reference, part of the laser radiation was directed to an additional cell (*2*) filled with Rb vapors, whose absorption at the $1, 2 \to 1', 2'$ transitions of the ^{87}Rb atom and $2, 3 \to 2', 3'$ atom ^{85}Rb (Fig. 2) served as a frequency reference. In some cases, a nano-cell (NC) filled with Rb atom vapor with a vapor column thickness of $L \sim 400$ nm was placed instead of the (*2*) cell to form the frequency reference.

2. Results and discussion

In Fig. 3, the upper curve shows the FL spectrum of Rb vapor in a conventional cell $L = 2$ cm, $P = 1$ mW. Since the Doppler width of atomic transitions is ~ 500 MHz, and the frequency distance between transitions ^{85}Rb is 362 MHz, they is no frequency separation. The top inset shows the fitting of transitions ^{85}Rb by Gaussian curves for transitions $2 \to 2', 3'$ with the relative probabilities shown in Fig. 2. The ratio of peak amplitudes of FL atoms ^{85}Rb for transitions $A(2-3')/A(2-2') = 3.5$, and the ratio of peak amplitudes of FL atoms ^{87}Rb for transitions $A(1-2')/A(1-1') = 5$. These ratios are given to compare these values in the case of a PDMS-coated Rb cell.

In Fig. 3, the bottom curve shows the FL spectrum of a nano-cell filled with Rb atom vapor with a vapor column thickness of $L \sim 400$ nm (NC heated to 110°C, $P = 5$ mW). As shown in [2], the use of NC allows a significant reduction in the Doppler broadening of atomic transitions, which allows their frequency separation. The main reason for the constriction is that the greatest contribution to absorption is made by atoms flying parallel to the NC walls and

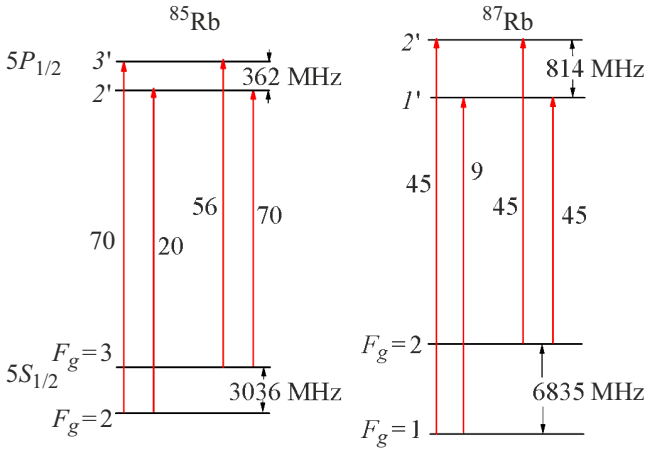

Figure 2. Diagram of levels and transitions for Rb atoms for the line D_1, transitions $5S_{1/2}-5P_{1/2}$, taking into account the hyperfine splitting of ground and upper levels (upper levels are marked with strokes). The arrows indicating the transitions are marked with their relative probabilities.

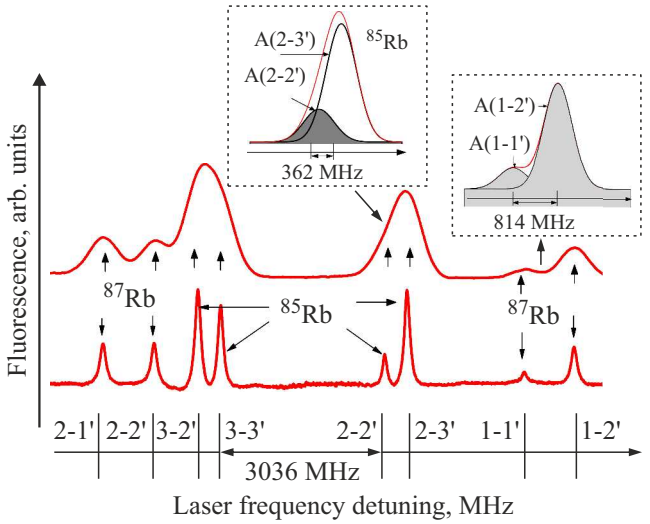

Figure 3. Upper curve — the FL spectrum of Rb vapor in a conventional centimeter cell, $P = 1$ mW. In the upper inset — fitting of transitions ^{85}Rb by Gaussian curves for transitions $3 \to 2', 3'$. FL peak amplitude ratio $A(2-3')/A(2-2') = 3.5$, FL peak amplitude ratio ^{87}Rb $A(1-2')/A(1-1') = 5$. Bottom curve — FL spectrum from NC with Rb vapor with vapor column thickness $L \sim 400$ nm, NC heated to 110°C. The use of NC allows the narrowing of atomic transitions and their frequency separation.

perpendicular to the direction of laser radiation propagation **k** (where **k**-wave vector). For such atoms, the Doppler shift in the frequency of atomic transitions is small. At the same time, atoms flying along the laser radiation propagation **k** experience inelastic collisions with the NC walls (the transit time to the walls for atoms with average thermal speed is only a few nanoseconds) and are nonradiative at the lower levels of ^{87}Rb, $F_g = 1, 2$ and ^{85}Rb, $F_g = 2, 3$. Consequently, the conditions for the atoms in the NC and in the anti-relaxation coated cell are diametrically opposite. It is also important to note that in the case of NC, the atomic transition amplitudes ^{87}Rb $1, 2 \to 1', 2'$ and ^{85}Rb $2, 3 \to 2', 3'$ correspond well to the relative probabilities shown in Fig. 2.

Fig. 4 top curve 1 shows the FL spectrum of Rb vapor in a PDMS cell, laser power $P = 4.9$ mW, intensity $I = 220\,\text{mW}\cdot\text{cm}^{-2}$ (saturation intensity for atoms ^{87}Rb and ^{85}Rb is $\sim 4.5\,\text{mW/cm}^2$ [23]). The result is quite unexpected, because in the transmission (absorption) spectrum shown on the middle curve, there are no atomic lines at the transitions of atoms ^{87}Rb, ^{85}Rb, but there is absorption (without substructure) at several percent level. The results for the transmittance spectrum agree with the results of [20], which also used a PDMS-coated Rb cell and in which the effect of hyperfine optical pumping began to appear as the laser intensity increased. Resonant laser radiation transfers atoms from, the first ground level to the upper excited levels, from which atoms spontaneously move to the second ground level. Since the frequency distances between the ground levels are quite large — 3 and 6.8 GHz respectively for the atom ^{85}Rb and ^{87}Rb (Fig. 2) — the laser frequency is no longer in resonance with the atomic

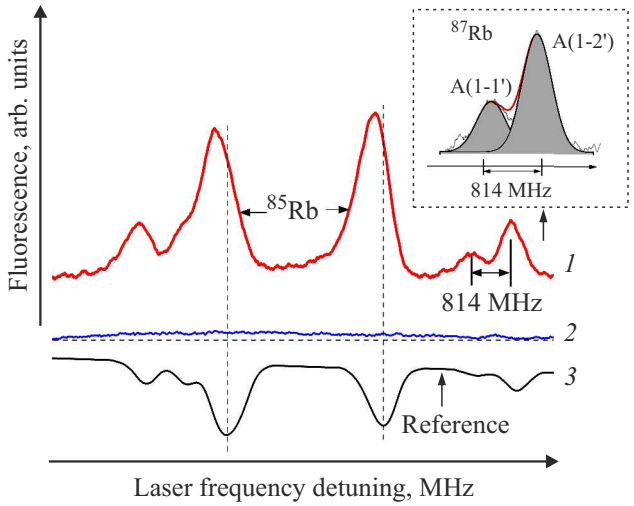

Figure 4. The upper curve (*1*) —the FL spectrum of Rb vapor in the PDMS cell, $P = 4.9$ mW, $I = 220\,\text{mW/cm}^2$. In the inset — fitting of transitions ^{87}Rb by Gaussian curves for the ratio of amplitudes FL $A(1-2')/A(1-1') \sim 2.2$; the middle curve (*2*) — the transmission (absorption) spectrum, where the atomic lines at the ^{87}Rb, ^{85}Rb transitions are missing. The bottom curve (*3*) — the reference (reference) — the transmission spectrum of a normal two-centimeter Rb cell.

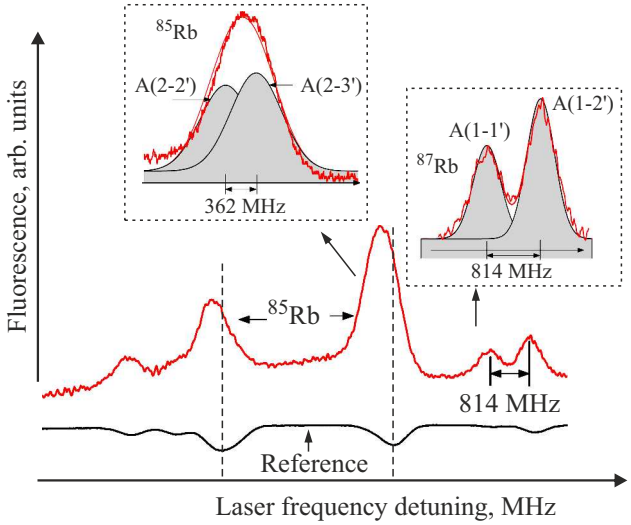

Figure 5. The upper curve — FL of Rb vapor in PDMS cell, $P = 8.5$ mW, $I \sim 380\,\text{mW/cm}^2$. The inserts — fitting the transitions ^{85}Rb and ^{87}Rb by Gaussian curves for the transitions $2 \to 2', 3'$ and $1 \to 1', 2'$. Ratio of peak amplitudes of FL atoms ^{85}Rb $A(2-3')/A(2-2') \sim 1.14$, ratio of peak amplitudes of FL atoms ^{87}Rb $A(1-2')/A(1-1') \sim 1.5$.

transition from the second level. This results in tens of times lower absorption at atomic transitions at high laser intensities. This phenomenon is called optical pumping (OP) [21,24]. At high laser intensities (Fig. 4.), there is a strong deformation of the ^{85}Rb, ^{87}Rb spectra profiles compared to the reference spectra (lower curve) and a frequency shift of peak amplitudes (dashed vertical lines show the unbiased position of peak amplitudes ^{85}Rb). The inset shows the fitting of transitions ^{87}Rb by Gaussian curves for transitions $1 \to 1', 2'$. The ratio of the peak amplitudes of FL atoms ^{87}Rb for transitions $A(1-2')/A(1-1') \sim 2.2$ (from the diagram shown in Fig. 2, this ratio should be 5). There is also a change in the FL peak amplitude ratio of the atoms ^{85}Rb for the transitions $2 \to 2', 3'$, which is evident in the FL spectrum at higher laser intensity, shown in Fig. 5. Changing the ratio for the atomic transition amplitudes leads to a frequency shift of the peak envelope amplitudes, which is observed better for ^{85}Rb atoms, since the frequency distance between transitions (362 MHz) is significantly smaller than for ^{87}Rb.

The OP efficiency [24] process is determined by the expression

$$\eta \sim \frac{\Omega^2 \gamma_N t}{(\Delta + \mathbf{kv})^2 + \Gamma^2}, \qquad (1)$$

where $\Omega = Ed/h$ — Rabi frequency, E — electric field of radiation, d — dipole moment, t — interaction time of radiation with atom, **kv** — Doppler shift, Δ — frequency shift from resonance, Γ is the sum of homogeneous and inhomogeneous broadenings. The Rabi frequency (with nice accuracy) can be determined from the expression $\Omega/2\pi = \gamma_N (I/8)^{1/2}$ [25] where I laser intensity expressed in $\text{mW}\cdot\text{cm}^{-2}$, γ_N as in formula (1) — radiation width

of excited state. As can be seen from formula (1), the OP efficiency is strongly dependent on the Rabi frequency, i. e., on I. At small $I \sim 1\,\text{mW}\cdot\text{cm}^{-2}$ the OP process is virtually absent, and the transmission spectrum of the PDMS cell repeats that of an uncoated cell —the lower reference curve *3* in Fig. 4. Formula (1) shows that the longer the interaction time t, the higher the OP efficiency. This is confirmed by work [20]: decreasing the scanning frequency of the laser frequency down to a few Hz led to a decrease in absorption at atomic transitions by a factor of ten compared to the case when the scanning frequency was large. The FL process has not been investigated in work [20] and, to our knowledge, there is only one paper that has investigated the FL damping time in a cell with a carefully prepared [26] surface prior to coating. In Fig. 5, the upper curve shows the FL spectrum of Rb vapor in the PDMS cell, laser power 8.5 mW, intensity $\sim 380\,\text{mW/cm}^2$; the transmission spectrum is similar to the transmission spectrum in Fig. 4 (curve *2*), that is there are no atomic lines at transitions of atoms ^{87}Rb, ^{85}Rb, while there is absorption (without substructure) at several percent level (transmission spectrum in Fig. 5 is not shown). With increasing laser intensity, there is a stronger deformation of the ^{85}Rb and ^{87}Rb spectra profiles compared to the reference spectra (bottom curve), and there is a significant frequency shift of 200–250 MHz peak amplitudes relative to the dotted line, which shows an unbiased position. The insets show the fitting of transitions ^{85}Rb and ^{87}Rb by Gaussian curves for transitions $2 \to 2', 3'$ and $1 \to 1', 2'$. The ratio of peak amplitudes of FL atoms ^{85}Rb for transitions $\text{A}(2-3')/\text{A}(2-2') \sim 1.14$ (according to the diagram of Fig. 2 should be 3.5), and the ratio of peak fluorescence amplitudes of atoms ^{87}Rb for transitions $\text{A}(1-2')/\text{A}(1-1') \sim 1.5$ (according to the diagram of Fig. 2 should be 5). A change in the ratio for the amplitudes of atomic transitions leads to a frequency shift in the peak amplitudes of the envelopes. Since for the marked transitions ^{85}Rb (^{87}Rb), the lower level is the same $F_e = 2$ ($F_g = 1$), its population increase or decrease due to the OP presence, occupation of upper levels $F_e = 2, 3$ ($F_e = 1, 2$), from which FL occurs, and the ratio of their amplitudes should not have changed, while FL increases stronger from the level below, $F_e = 2$ ($F_e = 1$). A possible explanation for the FL features is as follows.

A feature of Rb atoms (compared to other alkali metal atoms) is the presence of quasi-resonance during two-photon excitation by the same photons with $\lambda = 795\,\text{nm}$ at the $5S-5D_{3/2}$ [27,28] transition. Since the ionization energy of the Rb atom is $33\,690\,\text{cm}^{-1}$ [22], and the photon energy with $\lambda = 795\,\text{nm}$ is $12\,580\,\text{cm}^{-1}$, three photons energy is sufficient for ionization (the presence of a two photon resonance increases the ionization probability). The work [29] shows that the $5D$ level can also be populated by an effect called energy pooling, whereby of two excited atoms at the $5P$ level, one atom goes to the excited $5D$ level after collision, while the other is at the lower $5S$ level. Since the energy of the level $5D_{3/2}$ is $25700\,\text{cm}^{-1}$, one photon with $\lambda = 795\,\text{nm}$ is sufficient for the subsequent one-photon ionization. In work [30], the ionization of Rb atoms during two-photon resonance was investigated using a dye laser by detectable photoionization current. The Rb ion formed as a result of ionization captures a free electron and recombination occurs, as a result of which, the atom is at the upper excited levels. Fig. 6 shows a diagram based on the results of the work [27,28], showing with arrows how the level $5P_{1/2}$ can be populated by spontaneous decay from above levels $nS_{1/2}$, where $n = 6, 7, 8, 9$, and $nD_{3/2}$, where $n = 6, 7, 8$. A thin 2 mm-glass Rb-cell heated to 160°C was used. At this temperature, the Rb atoms begin to displace the silicon atoms from the glass (SiO_2), which precipitate on the inner surface of the cell, causing its windows to darken. It is important to note that in [27,28] emission wavelengths in the 400–900 nm range were recorded at the transitions of Rb atoms to the $5P_{1/2}$ level, from which fluorescence occurs. The same authors recorded blue radiation (in Fig. 6, marked with b) with $\lambda = 422\,\text{nm}$, transition $6P_{1/2} \to 5S_{1/2}$, indicating that the $5D$ level (from which one-photon ionization of the atom can also take place) is populated with a further transition of the atom to the $6P_{1/2}$ level. From work [27], it follows that in some cases the level $5P_{1/2}$ is populated by transitions from the upper levels $nS_{1/2}$ and $nD_{3/2}$ better than the level $5P_{3/2}$ located above, which could also be an explanation for the fact that the fluorescence from the lower levels of the atoms ^{85}Rb $F_e = 2$ and ^{87}Rb $F_e = 1$ increases more strongly.

The above mentioned mechanism of FL occurrence is also indicated by the fact that FL from the PDMS cell is several times less than from the conventional Rb cell under the same conditions, since the number of ionized Rb atoms can be no more than 20–30% of the total number of atoms participating in the settlement of the $6P_{1/2}$ level by direct

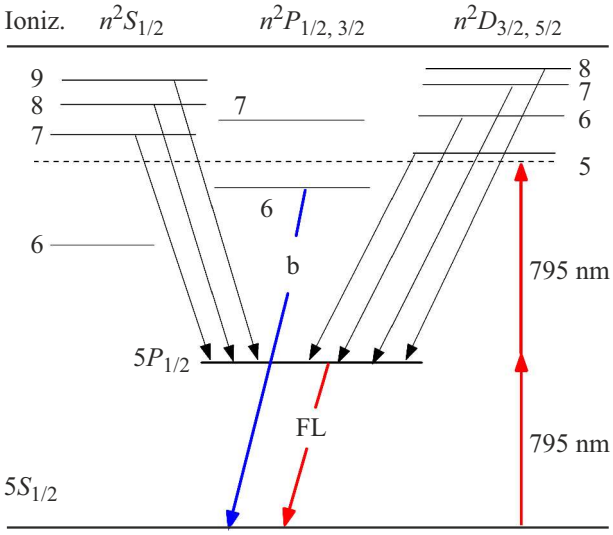

Figure 6. Diagram of the Rb atom levels, based on the results of [27,28]. The atomic levels are not to scale. Only those levels are given that are necessary to explain the $5P_{1/2}$ level settlement from which fluorescence (FL) occurs. The energy of the atomic level ($33\,690\,\text{cm}^{-1}$), above which ionization occurs (marked on the ioniz diagram).

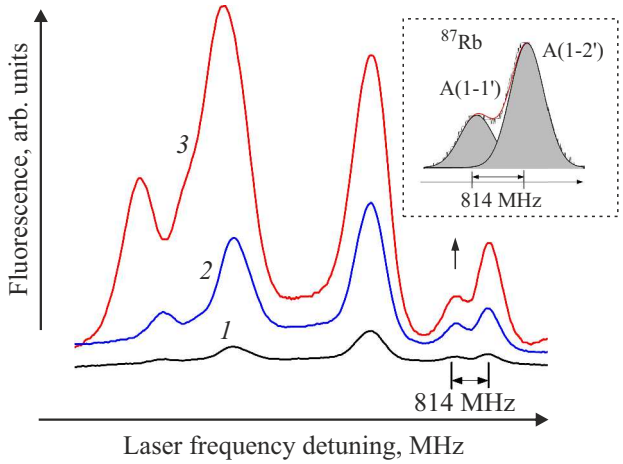

Figure 7. Curves *1, 2* and *3* – the spectra of FL at temperatures 20, 35 and 45°C, respectively. The FL intensities at atomic transitions are redistributed: in the inset — fitting of transitions ^{87}Rb by Gaussian curves for transitions $1 \to 1', 2'$. FL peak amplitude ratio ^{87}Rb $A(1-2')/A(1-1') \sim 2.5$, at room temperature ratio 1.5.

absorption from the main lower levels in the conventional Rb cell. Nevertheless, we do not exclude the presence of an additional mechanism for populating the $5P_{1/2}$ level in the PDMS cell with the subsequent FL.

The dependence of FL in the PDMS cell on temperature was investigated. The *1, 2* and *3* curves in Fig. 7 show the FL spectra at temperatures 20, 35, and 45°C, at which the Rb atomic density is $\sim 4 \cdot 10^9$, $2 \cdot 10^{10}$, $9 \cdot 10^{10}$ cm^{-3}, respectively. Note, that the FL intensities at atomic transitions are redistributed as the density increases: the box shows the fitting of the transitions ^{87}Rb by the Gaussian curves for the transitions $1 \to 1', 2'$. The peak amplitude ratio of FL atoms ^{87}Rb for transitions $A(1-2')/A(1-1') \sim 2.5$, while in the PDMS cell at room temperature (Fig. 5), the peak amplitude ratio was 1.5. This is due to the fact that as the density of atoms increases due to Rb–Rb collisions, the atoms speed in the cell decreases up to the diffusion rate at high densities [23], therefore, the atoms „feel weaker" the cell walls and the presence of a coating on them.

Since coated cells are currently in active use [18], we hope that the above research will be useful.

3. Conclusion

To suppress inelastic collisions of atoms with cell walls, cells with anti-relaxation organic coatings on the inner walls are now widely used. In the work, we investigated the peculiarities of the Rb vapor fluorescence spectra of the D_1 line using a PDMS-coated cell. In common cells filled with alkali metal vapor, the absorption and fluorescence spectra are almost identical. In the work, it is shown that in the PDMS cell in the transmission spectra of intense (> 220 mW/cm^2) laser radiation due to the effect of optical pumping of Rb atoms, the D_1 absorption lines at atomic transitions are almost absent, while in the fluorescence spectrum, all 8 atomic transitions D_1 lines are strongly pronounced. A physical explanation for this difference in spectra is given. The FL spectrum registers a strong redistribution of intensity at atomic transitions ^{85}Rb and ^{87}Rb: thus, the ratio of peak fluorescence amplitudes of atoms ^{85}Rb for transitions $2 \to 2', 3'$ (for ^{87}Rb, $1 \to 1', 2'$) in a normal cell is $A(2-3')/A(2-2') = 3.5$ (for ^{87}Rb is the ratio $\tilde{5}$), and in PDMS-cell $A(2-3')/A(2-2') \sim 1.14$ (for ^{87}Rb ratio $A(1-2')/A(1-1') \sim 1.5$). Increasing the temperature of the PDMS cell increases the fluorescence of the rubidium atoms, but the spectra show some redistribution of intensities at the atomic transitions ^{85}Rb and ^{87}Rb. Thus, when using coated cells and intense laser radiation, transmission (absorption) spectra contain almost no useful information about atomic transitions, since there are no absorption lines at atomic transitions, while fluorescence spectra are informative and can be used, in particular, to study the effect of a magnetic field on atomic transitions Rb.

Funding

The research of the authors A.S. and D.S. was carried out with the financial support of the Committee on Science of the Republic of Armenia within the scientific project № 21T-1C005.

Conflict of interest

The authors declare that they have no conflicts of interest.

References

[1] D. Pizzey, J. Briscoe, F. Logue, F. Ponciano-Ojeda, S. Wrathmall, I. Hughes. New J. Phys., **24**, 125001 (2022). DOI: 10.1088/1367-2630/ac9cfe
[2] A. Sargsyan, A. Amiryan, Y. Pashayan-Leroy, C. Leroy, A. Papoyan, D. Sarkisyan. Opt. Lett., **44**, 5533 (2019). DOI: 10.1364/OL.44.005533
[3] A. Sargsyan, E. Klinger, C. Leroy, T.A. Vartanyan. Opt. i spectr., **125**, 833–838 (2018).
[4] Z. Ding, X. Long, J. Yuan, Z. Fan, H. Luo. Sci. Rep., 6, 32605 (2016). DOI: 10.1038/srep32605
[5] E.B. Alexandrov, M.V. Balabas. Opt. i spectr., **98**, 879 (2005) (In Russian).
[6] W. Happer. Rev. Mod. Phys., **44**, 169 (1972). DOI: 10.1103/RevModPhys.44.169
[7] M.A. Bouchiat, J. Brossel. Phys. Rev., **147**, 41 (1966). DOI: 10.1103/PhysRev.147.41
[8] M.T. Graf, D.F. Kimball, S.M. Rochester, K. Kerner, C. Wong, D. Budker. Phys. Rev. A, **72**, 023401 (2005). DOI: 10.1103/PhysRevA.72.023401
[9] M.V. Balabas, T. Karaulanov, M.P. Ledbetter, D. Budker. Phys. Rev. Lett., **105**, 070801 (2010). DOI: 10.1103/PhysRevLett.105.070801
[10] M. Stephens, R. Rhodes, C. Wieman. J. Appl. Phys., **76**, 3479 (1994). DOI: 10.1063/1.358502
[11] V. Coppolaro, N. Papi, A. Khanbekyan, C. Marinelli, E. Mariotti, L. Marmugi, L. Moi, L. Corradi, A. Dainelli, H. Arigawa, T. Ishikawa, Y. Sakemi, R. Calabrese, G. Mazzocca,

L. Tomassetti, L. Ricci. J. Chem. Phys., **144**, 134201 (2014). DOI: 10.1063/1.4896609
[12] S.J. Seltzer, M.V. Romalis. J. Appl. Phys., **106**, 114906 (2009). DOI: 10.1063/1.3236649
[13] K. Nasyrov, S. Gozzini, A. Lucchesini, C. Marinelli, S. Gateva, S. Cartaleva, L. Marmugi. Phys. Rev. A, **92**, 043803 (2015). DOI: 10.1103/PhysRevA.92.043803
[14] A.N. Litvinov, G.A. Kazakov, B.G. Matisov. J. Phys. B, **42**, 165402 (2009). DOI: 10.1088/0953-4075/42/16/165402
[15] S.N. Atutov, V. Biancalana, P. Bicchi, C. Marinelli, E. Mariotti, M. Meucci, A. Nagel, K. Nasyrov, S. Rachini, L. Moi. Phys. Rev. A, **60**, 4693 (1999). DOI: 10.1103/PhysRevA.60.4693
[16] Y. Dancheva, C. Marinelli, E. Mariotti, L. Marmugi, M.R. Zampelli, P.N. Ghosh, S. Gateva, A. Krasteva, S. Cartaleva. J. Phys.: Conf. Ser., **514**, 012029 (2014). DOI: 10.1088/1742-6596/514/1/012029
[17] L. Marmugi, S. Gozzini, A. Lucchesini, A. Bogi, A. Burchianti, C. Marinelli. J. Opt. Soc. Am. B, **29**, 2729 (2012). DOI: 10.1364/JOSAB.29.002729
[18] E. Talker, P. Arora, R. Zektzer, Y. Sebbag, M. Dikopltsev, U. Levy. Phys. Rev. Appl., **15**, L051001 (2021). DOI: 10.1103/PhysRevApplied.15.L051001
[19] M. Bhattarai, V. Bharti, V. Natarajan, A. Sargsyan, D. Sarkisyan. Phys. Lett. A, **383**, 91 (2019). DOI: 10.1016/j.physleta.2018.09.036
[20] A. Krasteva, E. Mariotti, J. Dancheva, K. Marinelli, L. Marmugi, L. Staccini, S. Godzini, S. Gateva, S. Kartaleva. Journal of Contemporary Physics (Armenian Academy of Sciences) **55**, 383–396 (2020).
[21] W. Demtröder. *Laser spectroscopy: basic concepts and instrumentation* (Springer, 2004).
[22] D. Sarkisyan, T. Varzhapetyan, A. Sarkisyan, Yu. Malakyan, A. Papoyan, A. Lezama, D. Bloch, M. Ducloy. Phys. Rev. A, **69**, 065802 (2004). DOI: 10.1103/PhysRevA.69.065802
[23] https://steck.us/alkalidata (revision 2.2.2. 9 July, 2021)
[24] G.V. Nikogosyan, D.G. Sarkisyan, Yu.P. Malakyan. Journal of optical technology. **71** (9), 602–607 (2004).
[25] A. Sargsyan, C. Leroy, Y. Pashayan-Leroy, R. Mirzoyan, A. Papoyan, D. Sarkisyan. Appl. Phys. B, **105**, 767 (2011). DOI: 10.1007/s00340-011-4614-0
[26] S.N. Atutov, V.A. Sorokin, S.N. Bagayev, M.N. Skvortsov, A.V. Taichenachev. Eur. Phys. J. D, **73**, 240 (2019). DOI: 10.1140/epjd/e2019-100206-5
[27] L. Weller, R.J. Bettles, C.L. Vaillant, M.A. Zentile, R.M. Potvliege, C.S. Adams, I.G. Hughes. http://arxiv.org/abs/1308.0129v1
[28] L. Weller. *Absolute Absorption and Dispersion in a Thermal Rb Vapour at High Densities and High Magnetic Fields* (Doctoral thesis, Durham University, 2013).
[29] J. Keaveney, A. Sargsyan, D. Sarkisyan, A. Papoyan, C.S. Adams. J. Phys. B, **47**, 075002 (2014). DOI: 10.1088/0953-4075/47/7/075002
[30] C.B. Collins, S.M. Curry, B.W. Johnson, M.Y. Mirza, M.A. Chellehmalzadeh, J.A. Anderson. Phys. Rev. A, **14**, 1662 (1976). DOI: 10.1103/PhysRevA.14.1662

Translated by Y.Deineka